

ω	is the circular frequency of voltage supplied to sensor, sec^{-1} ;
μ	is the magnetic permeability of the medium;
v	is the local stream velocity beyond the limits of the boundary layer at the surface of the sensor head, cm/sec ;
V	is the velocity of the undisturbed stream, cm/sec ;
x	is the distance from center of the microelectrode along the surface of the head, cm ;
f	is the designation of functional dependence α ;
λ	is the coefficient of thermal conductivity of water;
ν	is the kinematic viscosity;
σ_*	is the electrical conductivity of water at the base temperature t_* ;
b	is the temperature coefficient of electrical conductivity.

LITERATURE CITED

1. A. Okubo, Oceanic Mixing, Mgmt. Info. Serv. (1970).
2. V. S. Belyaev, A. S. Monin, R. V. Ozmidov, and V. T. Paka, "Experimental investigation of fine-scale turbulence in the ocean," *Izv. Akad. Nauk SSSR, Fiz. Atmos. Okeana*, 10, No. 9 (1974).
3. J. O. Hinze, Turbulence, McGraw-Hill (1959).
4. H. Kramers, *Physica*, 12, 61 (1946).
5. H. Gröber, S. Erk, and U. Grigull, Principles of the Study of Heat Exchange [Russian translation], IL, Moscow (1958).
6. I. N. Tetel'baum, Electrical Modeling [in Russian], Fizmatgiz, Moscow (1959).
7. L. G. Loitsyanskii, Mechanics of Liquid and Gas, Pergamon (1965).
8. V. V. Skorshelletti, Theoretical Electrochemistry [in Russian], Khimiya, Leningrad (1969).

DESCRIPTION OF OPERATION OF JET GAS - LIQUID PUMP IN THE APPROXIMATION OF A NONEQUILIBRIUM MULTIPHASE-FLOW MODEL

S. D. Frolov

UDC 532.529:533.6

A description of the operation of a jet gas-liquid pump is obtained; the agreement between the results of calculation and experiment is satisfactory.

The jet gas-liquid pump (JGLP), proposed initially as a starting device for liquid metal MHD equipment [2] and then as a rocket-motor fuel pump [3], has not found its expected applications because of its low efficiency. However, as shown by more recent research [13], despite the highly dissipative energy transformations characteristics of all jet apparatus, the JGLP efficiency may be significantly increased.

The optimum organization of JGLP operation in each specific application requires the adequately complete and reliable description of its operation.

The JGLP operation may be represented schematically as follows (Fig. 1).

The quasihomogeneous gas (vapor)-liquid mixture formed in mixer 1 or the liquid heated to saturation point is accelerated in the two-phase nozzle 2 with slight and monitored slip between the phases. The acceleration of the liquid is mainly due to the action of aerodynamic forces from the carrier gas. Not only momentum transfer between the phases but also heat and mass transfer are possible. After the separation of the liquid in the high-velocity separator 4 its kinetic energy is transformed into the potential energy of pressure forces in the diffusor 5. Because of the presence of some of the carrier gas in the separated liquid, the flow in the diffusor is of bubble structure. Phase transformations may also occur in the diffusor.

Translated from *Inzhenerno-Fizicheskii Zhurnal*, Vol. 35, No. 5, pp. 834-841, November, 1978. Original article submitted October 24, 1977.

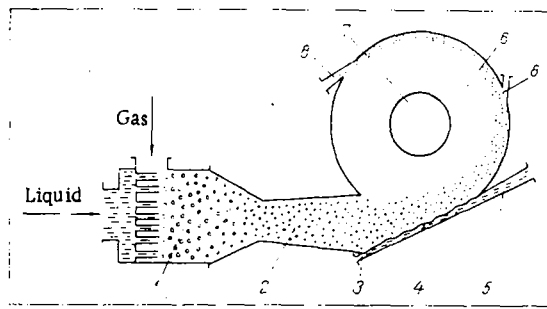


Fig. 1. Jet gas-liquid pump (JGLP): 1) mixer; 2) two-phase nozzle; 3) slit for liquid reinjection; 4) high-velocity separator; 5) diffuser; 6) secondary separator; 7) exhaust pipe; 8) secondary-separator trap.

Before exhaust, the carrier gas is pumped into the secondary separator 6. The liquid separated in 6 is fed from traps 8 and 3 to the main-separator inlet.

Thus, over practically the whole JGLP channel there moves a two-phase flow, in which energy is converted from one form to another and, in general, the situation is also complicated by phase transformations.

Attempts have been made to describe the operation of jet equipment using the equilibrium model of a two-phase medium [1]. This approach gives a sufficiently simple calculation procedure for the JGLP, but the reliability of the calculations depends on the accuracy with which the loss coefficients in the individual elements of the pump are specified.

Investigations of the basic jet-pump elements have shown the loss coefficients vary over a wide range, depending on the parameters of the process. Moreover, even with the appropriate choice of loss coefficients, the equilibrium method does not allow the detailed geometry of the flow part of the pump to be obtained; this is only possible from data on the actual phase-dependence distribution over the length of the flow part, which the equilibrium model cannot provide.

These requirements are met, to a considerable extent, by the nonequilibrium model of multiphase flow [4-6].

In addition to the usual assumptions of the nonequilibrium model [6], the following simplifications will be made:

that the flow, overall, is one-dimensional and steady;

that the discrete phase is distributed in the carrier phase as spherical drops or bubbles of equal size, which do not interact directly with one another, deviations from spherical form being taken into account only in determining the aerodynamic-drag coefficient of the disperse particles;

that, in the general case, one of the phases is an equilibrium vapor-gas mixture and the other an incompressible liquid;

that the carrier-phase viscosity only appears in the immediate vicinity of the phase interface and the channel walls.

that the gas phase as a whole, and also its components, satisfy the equations of state of a thermally and calorically perfect gas;

that, in general, phase transformations are nonequilibrium;

that the mechanical and thermodynamic properties of the phase, except the nature of the materials, depend only on the temperature;

that the radiant heat transfer between the phases and with the channel walls is very small.

Following [5], making the given assumptions, the system of basic equations may be written as follows: momentum equations for the carrier and discrete phases

$$\alpha_1 \rho_1^0 \omega_1 \frac{d\omega_1}{dz} = -\alpha_1 \frac{dp_1}{dz} - I(\omega_{12} - \omega_1) - (X_{12} - XF_1); \quad (1)$$

$$\alpha_2 \rho_2^0 w_2 \frac{dw_2}{dz} = -\alpha_2 \frac{dp_2}{dz} - I(w_{21} - w_2) + (X_{12} - X_{F2}), \quad (2)$$

where

$$I = \frac{1}{f} \cdot \frac{dm_1}{dz};$$

$$X_{12} = X_f + X_m;$$

$$X_f = \frac{3}{4} \bar{C}_2 \alpha_2 \frac{\rho_1^0}{\delta_p} |w_1 - w_2| (w_1 - w_2);$$

$$X_m = \frac{1}{2} \alpha_2 \rho_1^0 \frac{w_2}{\delta_p^3} \frac{d}{dz} [\delta_p^3 (w_1 - w_2)];$$

$$X_{\pi i} = 2 \bar{C}_{f i} \frac{m_i w_i}{f D_G};$$

$$w_{12} = w_{21} = \begin{cases} w_1 & \text{when } dm_2 \geq 0; \\ w_2 & \text{when } dm_2 < 0; \end{cases}$$

the heat-input equations for the carrier and discrete phases

$$\alpha_1 \rho_1^0 w_1 \frac{du_1}{dz} = \frac{\alpha_1 \rho_1 w_1}{\rho_1^0} \frac{d\rho_1^0}{dz} + X_{12} (w_1 - w_2) +$$

$$+ X_{F1} w_1 + I \frac{(w_{12} - w_1)^2}{2} + I \psi_{s1} - I c_{p1} (T_1 - T_{s1}) + I (c_{p2} T_2 - c_{ps2} T_{s2}) - q_{12} + \alpha_1 \rho_1^0 Q_1;$$

$$\alpha_2 \rho_2^0 w_2 \frac{du_2}{dz} = \frac{\alpha_2 \rho_2 w_2}{\rho_2^0} \frac{d\rho_2^0}{dz} - I \frac{(w_{21} - w_2)^2}{2} + I \psi_{s2} + I c_{p2} (T_2 - T_{s2}) - I (c_{p1} T_1 - c_{ps1} T_{s1}) + q_{12}, \quad (4)$$

where

$$q_{12} = 6 \alpha_T \tau_2 (T_1 - T_2) / \delta_p;$$

$$Q_1 = 4 \alpha_w (T_w - T_1) / \alpha_1 \rho_1^0 D_G;$$

$$\psi_{si} = \begin{cases} 0 & \text{when } dm_i \leq 0; \\ a_{i6} + a_{i7} T_{si} + a_{i8} T_{si} & \text{when } dm_i > 0; \end{cases}$$

$$T_{si} = a_0 + a_{12} \rho_i^{0.25};$$

the equation relating the mass-transfer rate and the particle size

$$\frac{1}{2} w_2 \frac{d\delta_p}{dz} = - \frac{I}{\pi \delta_p^2 n \rho_2^0}; \quad (5)$$

the thermal and caloric equations of state for the components of the carrier and discrete phases

$$p_i = \rho_i^0 R_i T_i; \quad (6)$$

$$u_i = (c_{pi} - R_i) T_i; \quad (7)$$

the mass-conservation equation for the two-phase flow

$$dm_1 + dm_2 = 0; \quad (8)$$

the equation of mass-transfer between the phases

$$\frac{dm_2}{dz} = 6 \alpha_n \frac{m_2}{\rho_2^0 \delta_p} (\rho_V - \rho_V^0); \quad (9)$$

the equation relating the phase pressures

$$p_2 - p_1 = 4\sigma / \delta_p; \quad (10)$$

the mass-flow-rate equations of the components of the two-phase flow

$$m_1 = \rho_1^0 f_1 w_1; \quad (11)$$

$$m_2 = \rho_2^0 f_2 w_2; \quad (12)$$

the area-balance equation

$$f = f_1 + f_2; \quad (13)$$

the closing equation is taken in a form convenient for both nozzle and diffuser flow

$$p_1 = a_{27} + a_{28}z + a_{29}z^2. \quad (14)$$

The adequacy of this calculation model depends considerably on the reliability with which the coefficients of momentum, heat, and mass transfer at both the phase interfaces and the flow boundaries appearing in the equations are determined.

The force-interaction coefficient between the phases is calculated from the relations obtained in [7], taking into account the recommendations of [8]

$$\bar{C}_z = C_z \alpha_1^{-n_z}; \quad (15)$$

$$C_z = \begin{cases} \frac{24}{\text{Re}_p} + \frac{2.5}{\text{Re}^{0.25}} \text{ when } \text{Re}_p \leq 4.55 A^{0.21}; \\ 0.73 \text{Re}_p^{1.4} A^{-0.4} \text{ when } \text{Re}_p > 4.55 A^{0.21}; \end{cases} \quad (16)$$

$$A = \sigma^3 (\rho_1^0)^2 / 9.81 (\mu_1^0)^4 (\rho_2^0 - \rho_1^0); \quad (17)$$

$$\text{Re}_p = |\omega_1 - \omega_2| \rho_1^0 \delta_p^0 \mu_1^0. \quad (18)$$

The frictional coefficients of the phases at the channel wall are determined from the relations [9]

$$\bar{C}_{fi} = C_{fi} \alpha_i^{-n_z}; \quad (19)$$

$$C_{fi} = \begin{cases} 16 \text{Re}_i \text{ when } \text{Re}_i < 2 \cdot 10^3; \\ 0.0791 \text{Re}_i^{0.25} \text{ when } 2 \cdot 10^3 > \text{Re}_i > 10^5; \end{cases} \quad (20)$$

$$\text{Re}_i = \rho_i^0 \omega_i D_{Hi}^0 \mu_i^0. \quad (21)$$

The interphase heat-transfer coefficient is given by the generalizing relation

$$\alpha_T = (a_{19} + a_{20} \text{Pr}^{1/3} \text{Re}_p^{1/2}) \lambda \delta_p, \quad (22)$$

which, for appropriate values of a_{19} and a_{20} , expresses the particular formulas proposed by various authors; in this expression

$$\text{Pr} = c_p \mu / \lambda;$$

$$\lambda = g_V \lambda_V + (1 - g_V) \lambda_G;$$

$$c_p = g_V c_{pV} + (1 - g_V) c_{pG};$$

$$\mu = g_V \mu_V + (1 - g_V) \mu_G;$$

$$g_V = m_V / (m_V + m_G).$$

The heat-transfer coefficient between the walls and the carrier phase is given by a relation analogous to Eq. (22)

$$\alpha_w = (a_{19} + a_{20} \text{Pr}_1^{1/3} \text{Re}_1^{1/2}) \frac{\lambda_1}{D_G}. \quad (23)$$

The interphase mass-transfer coefficient is related to the mutual-diffusion coefficient D in the vapor-gas mixture and other parameters as follows

$$\alpha_D = (a_{19} + a_{20} \text{Sc}^{1/3} \text{Re}_p^{1/2}) \frac{D}{\delta_p}. \quad (24)$$

TABLE 1. Comparison of Calculated and Experimental Results

Parameter			Calc.	Expt.	Equilibrium- method calc.	
Initial data	Liquid	Initial pressure	bar	6,66	6,86	6,66
		Temperature	°K	303	305	300
		Mass flow rate	kg/sec	2,3	2,44	2,5
	Gas	Initial pressure	bar	6,48	6,51	6,48
		Temperature	°K	323	355	300
		Mass flow rate	kg/sec	0,0852	0,0920	0,0833
		Degree of expansion of gas		4,33	4,29	4,33
Results obtained	Injection coefficient			27	26,5	30
	Separation coefficient		0,9	0,892	0,92*	
	Vol. gas content before diffusor		0,5	0,326	0,5	
	Liquid pressure at pump outlet		12,53	11,91	10,37	
	Isothermal pump eff. (%)		11,6	9,64	8,85	

*Specified as initial data in the equilibrium-model calculation.

where

$$D = D_0 (T/273)^{n3};$$

$$Sc = \mu/\rho D;$$

$$\rho = r_V \rho_V + (1 - r_V) \rho_G$$

$$r_V = m_V \left(m_V + \frac{x_V}{x_G} m_G \right).$$

The solution of Eqs. (1)-(24) reduces to numerical integration of a system of equations of the form

$$d\phi_j/dz = \Phi_j(z), \tag{25}$$

invariant for given initial data, for both nozzle and diffusor flow, regardless of the flow structure. On inversion of the flow structure (transition from droplet to bubble structure or the reverse), only the exchange of location (and the corresponding renotation of parameters) of the material in the carrier and disperse phases is taken into account.

The following parameter serves as an index of flow-structure inversion

$$\alpha_L = f_L/f. \tag{26}$$

When $\alpha_L < 0.26$ the two-phase flow is of droplet structure and when $\alpha_L \geq 0.26$ it is of bubble structure.

The separator calculation reduces to the solution of a system of equations describing the flow of a two-phase mixture in a curvilinear channel of given symmetry.

The actual flow pattern in the separator channel is very complex. The flow is known not to be one-dimensional. In the separator channel itself, the flow is clearly separated into a region of droplet structure and a region of bubble (foamlike) structure, between which there is no distinct boundary. In addition to the separation of drops with the formation of a moving film of separated liquid, inverse processes are also observed: breakaway and reflection of drops and also the introduction of gas bubbles with droplets entering the film. Therefore, the separator calculation necessitates the use of considerable simplifications and of empirical data.

A calculation model of the separation process in this formulation is given in [10].

As established experimentally, in some diffusor operating conditions the separated flow may be retarded before entry to the diffusor (may experience external compression). This leads to reduction in gas content at the diffusor inlet and to change in liquid velocity and pressure at this cross section, as well as pressure at the diffusor outlet.

To take account of external compression, it is necessary to have a set of experimental characteristics of the prototype separator

$$\begin{aligned}\alpha_{1I} &= F_1(\varepsilon_I, \delta_D); \\ \tau_E &= F_2(\varepsilon_I, \delta_D); \\ \sigma_E &= F_3(\varepsilon_I, \delta_D),\end{aligned}\quad (27)$$

using which corrected values may be obtained for the velocity w_{1E} and pressure p_{1E} at the end of the separator (the diffuser inlet) and the pressure p_{1D} after the diffuser, from the relations

$$\tau_E = (w_{1I}^2 - w_{1E}^2)(w_{1I}^2 - w_{1D}^2); \quad (28)$$

$$\frac{p_{1E} - p_{1O}}{0,5\rho_1^0 (w_{1I}^2 - w_{1E}^2)} = \sigma_E \left[1 + \frac{1}{u_D} - \frac{2R_2 T_2 \ln \frac{p_{1E}}{p_{1O}}}{u_D (w_{1I}^2 - w_{1E}^2)} \right]; \quad (29)$$

$$\frac{p_{1D} - p_{1E}}{0,5\rho_1^0 (w_{1E}^2 - w_{1D}^2)} = \sigma_D \left[1 + \frac{1}{u_D} - \frac{2R_2 T_2 \ln \frac{p_{1D}}{p_{1E}}}{u_D (w_{1E}^2 - w_{1D}^2)} \right]; \quad (30)$$

$$u_D = \rho_1^0 R_2 T_{1I} (1 - \alpha_{1I}) / \alpha_{1I} p_{1I}. \quad (31)$$

The actual volumetric bulk gas content of the flow at the end of the separator (the diffuser inlet) is given by the relation

$$\alpha_{1E} = \left(1 + \frac{u_D p_{1E}}{\rho_1^0 R_2 T_2} \right)^{-1}. \quad (32)$$

On the basis of the above model equations, a method was developed and a universal program written for the calculation of the flow parameters and geometry in the flow region of JGLP.

Detailed investigation of JGLP operation in individual elements of the pump confirm that the nonequilibrium model used for its description is of acceptable accuracy and efficiency [10-13].

Comparison of the integral JGLP parameters calculated by the given method with experimental values obtained in tests with the MSN-K-08 small-scale model operating with water + air (Table 1) also confirms this conclusion.

The results of the equilibrium-model calculation with similar initial data shown in Table 1 correspond to the following coefficients of mechanical-energy loss in the elements of the pump: $\sigma_N = 0.97$; $\varphi_N = 0.85$; $C_f = 0.02$; $\sigma_D = 0.92$.

From these data it follows that good agreement between the results of equilibrium-model calculations and experiment may only be obtained when the values of the loss coefficients are satisfactory.

NOTATION

w	is the velocity, m/sec;
p	is the pressure, N/m ² ;
ρ	is the density, kg/m ³ ;
T	is the temperature;
m	is the mass flow rate, kg/sec;
δ	is the particle diameter, height of diffuser slit;
α_i	is the volumetric fraction of mixture component i;
ψ_{si}	is the heat of phase transition of mixture component;
f	is the cross-sectional area of flow;
c	is the specific heat, J/kg · deg;
σ	is the surface tension, J/m ² ;
λ	is the thermal conductivity, W/m · deg;
μ	is the dynamic viscosity, N · sec/m ² ;
R_i	is the substantial gas constant, J/kg · deg;
D_H	is the hydraulic diameter of the flow, m;

a_j	are substantial constants ($j = 0, 1, 2, 3, \dots$);
z	is the coordinate, m;
σ_E	is the pressure-recovery coefficient under external compression;
σ_D	is the pressure-recovery coefficient in the diffuser;
ϵ	is the degree of separation;
π	is the degree of expansion (compression);
u	is the injection coefficient;
κ	is the molecular weight;
I	is the intensity of sources (sinks) of carrier-phase mass; $\text{kg/sec} \cdot \text{m}^3$;
X_{12}	is the phase-interaction force, incorporating the aerodynamic force X_f and the force X_m due to the "added"-mass effect, N;
X_{Ti}	is the frictional force between the phase and the channel wall, N;
q_{12}	is the interphase heat flow, W/m^2 ;
Q_1	is the external heat supply to carrier phase, W/kg .

Indices

1	is the carrier phase;
2	is the discrete phase;
R	is the radial component;
w	is the wall;
s	is the value at saturation;
G	is the gas;
V	is the vapor;
L	is the liquid;
P	is the particle;
$i = 1, 2$	is the phase number;
N	is the nozzle;
D	is the diffuser;
E	is the external compression;
0	is the exhaust (outlet) cross section;
I	is the primary separation;
°	is the actual value;
'	denotes the value corrected to the conditions far from the phase interface;
"	denotes the value corrected to the conditions at the phase interface.

LITERATURE CITED

1. Yu. N. Vasil'ev, in: Turbine Machines and Jet Equipment [in Russian], No. 5, Mashinostroenie (1971), p. 175.
2. D. J. Cerini, "Calculation of liquid for MHD-power generation," *Electr. MHD*, **3**, 2019 (1968).
3. D. Elliott, *Vopr. Raketn. Tekh.*, No. 4 (1964).
4. Kh. A. Rakhmatulin, *Prikl. Mat. Mekh.*, **20**, No. 2 (1956).
5. R. I. Nigmatulin, *Prikl. Mat. Mekh.*, **35**, No. 3 (1971).
6. A. N. Kraiko, R. I. Nigmatulin, V. K. Starkov, and L. E. Sterlin, "Mechanics of multiphase media," *Results of Science and Technology. Hydromechanics* [in Russian], Vol. 6, VINITI, Moscow (1972), p. 93.
7. A. S. Lyshevskii, *Izv. Vyssh. Uchebn. Zaved., Fiz., Mashinostr.*, No. 5 (1964).
8. N. I. Ivanenko, V. G. Selivanov, and S. D. Frolov, in: *Problems of Power-Station Gas Thermodynamics* [in Russian], No. 3, Kharkov Institute Aviation (1976).
9. S. D. Frolov, in: *Problems of Power-Station Gas Thermodynamics* [in Russian], No. 3, Kharkov Aviation Institute (1976), p. 53.
10. G. A. Gorbenko and S. D. Frolov, in: *Problems of Power-Station Gas Thermodynamics* [in Russian], No. 1, Kharkov Aviation Institute (1974), p. 107.
11. A. I. Borisenko, V. G. Selivanov, and S. D. Frolov, in: *Problems of Power Station Gas Thermodynamics* [in Russian], No. 1, Kharkov Aviation Institute (1974), p. 83.

12. V. G. Selivanov, K. I. Soplentov, and S. D. Frolov, in: Problems of Power Station Gas Thermodynamics [in Russian], No. 2, Kharkov Aviation Institute (1975), p. 19.
13. G. A. Gorbenko, V. G. Selivanov, K. I. Soplentov, and S. D. Frolov, in: Problems of Power-Station Gas Thermodynamics [in Russian], No. 2, Kharkov (1975), p. 88.

CHANGE IN THE NATURE OF HYDRODYNAMIC CAVITATION IN NONUNIFORM MAGNETIC FIELDS

N. F. Bondarenko, E. Z. Gak,
M. Z. Gak, and É. E. Rokhinson

UDC 663.631:538.651:532.575

It is known that in nonuniform magnetic fields the precavitation properties of aqueous media change, leading to an increase in the irreversible physicochemical changes.

The effect of magnetic fields on the physicochemical processes in aqueous media when there is hydrodynamic cavitation has not been investigated to any great extent. This problem is nevertheless of considerable practical interest for solving the problem of monitoring hydrodynamic cavitation. The results obtained in this paper show the leading part played by hydrodynamic factors in the mechanisms by which magnetic fields act on the properties of technical waters, and may be useful in constructing technological equipment and in choosing its mode of operation.

1. Vortex Formation and Dehydration in the Precavital Mode. Consider the flowing hydrodynamic system shown in Fig. 1. The length of region II is l , the diameter of the tubes in regions I and III is D , and the diameter of the tube in region II is d , $d < D$; p_I , p_{II} , p_{III} and V_I , V_{II} , V_{III} are the pressures and velocities in regions I, II, and III, respectively. The flow in region II is turbulent due to hydrodynamic factors and $Re = dV_{II}/\nu \geq Re_{cr}$.

A flowing system like this one in practice contains dissolved and free gases and microparticles. In 1 cm³ of natural water there are several hundreds of gas bubbles of diameter from 4 μ m to 30 μ m and up to $5 \cdot 10^5$ foreign particles of dimensions down to several microns [1]. Technical water contains different ions of electrolytes and has an electrical conductivity σ .

Suppose that in region II there is a nonuniform magnetic field represented by the induction \mathbf{B} and an induction gradient $\text{grad } \mathbf{B}$. We will also assume that $B = B_{\max}$ on the walls of the magnetic conductor, which is usually a component part of the hydroconductor. Satisfaction of the conditions $\text{grad } \mathbf{B} \neq 0$, $B \neq 0$ ensures that in region II in the volume of the liquid there will be induced nonuniform electric fields $\mathbf{E} = [\mathbf{V}_{II} \times \mathbf{B}]$ and $\text{grad } \mathbf{E} \neq 0$ leading to the occurrence in the volume of the liquid of induced currents of density $\mathbf{j}_i = \sigma[\mathbf{V}_{II} \times \mathbf{B}]$.

When considering flowing liquid media of low conductivity, the spatial distribution of the rotational forces which occur in the liquid under practical conditions [2] becomes of considerable importance. Hence, we will consider the phenomena that arise in aqueous media only when the conditions $\mathbf{j}_i \neq 0$, $\text{grad } \mathbf{B} \neq 0$ are satisfied, which automatically leads to the condition

$$\text{rot } \mathbf{f}_{\text{MHD}} = (\mathbf{B} \text{ grad}) \mathbf{j}_i - (\mathbf{j}_i \text{ grad}) \mathbf{B} \neq 0, \quad (1)$$

where

$$\mathbf{f}_{\text{MHD}} = [\mathbf{j}_i \times \mathbf{B}]. \quad (2)$$

Note that the effect of large-scale vortex formations in aqueous media when they flow through nonuniform magnetic fields is well known in the literature as an obstacle to the operation of magnetohydrodynamic (MHD) flowmeters [2].

Condition (1) ensures vorticity of the flow in space and time. Under turbulent conditions the values of the MHD forces in the boundary layers are determined not by the value of σ , but by σ_b , $\sigma \ll \sigma_b$ [3].

Agrophysical Institute, Leningrad. Translated from *Inzhenerno-Fizicheskii Zhurnal*, Vol. 35, No. 5, pp. 842-850, November, 1978. Original article submitted November 11, 1977.